Oct 17th, 12:00 AM

Modeling of Cold-formed Purlins-sheeting Systems

S. Kitipornchai

R. M. Lucas

F. G. A. Al-Bermani

Thirteenth International Specialty Conference on Cold-Formed Steel Structures
St. Louis, Missouri U.S.A., October 17-18, 1996

MODELING OF COLD-FORMED PURLINS-SHEETING SYSTEMS

R.M. LUCAS, F.G.A. AL-BERMANI and S. KITIPORNCHAI

Department of Civil Engineering, The University of Queensland
Brisbane, Qld 4072, Australia

SUMMARY

Purlin-sheeting systems used for roofs and walls commonly take the form of cold-formed channel or zed section purlins, screw-connected to corrugated sheeting. This paper presents two nonlinear elasto-plastic finite element models, capable of predicting the behaviour of purlin-sheeting systems without the need for either experimental input or over simplifying assumptions. The first model incorporates both the sheeting and the purlin while the second, a simplified version of the first model, includes only the purlin. Both models are able to account for cross-sectional distortion of the purlin, the flexural and membrane restraining effects of the sheeting, and failure of the purlin by local buckling or yielding. The validity of the models is shown by their good correlation with experimental results.

1 INTRODUCTION

Cold-formed steel zed and channel section members are widely used as purlins or girts, the intermediate members between the main structural frame and the corrugated roof or wall sheeting. In Australia, purlins are connected to the roof sheeting by way of a screw through the crest of the corrugated sheeting and the purlin flange. These cold-formed sections are generally thinner than hot-rolled members and hence behave differently to the heavier beams considered in standard steel design. The cross-sectional configurations of the zed and channel section purlins are such that they undergo both bending and twist from the beginning of loading. Due to the restraining action of the sheeting they tend to fail, not by overall flexural-torsional buckling, but by local plastic collapse, yielding or local buckling. Fig. 1 shows the general deflected shape of these purlins. The two purlins are shown under wind uplift loading which tends to be the dominant factor in Australian design.

The corrugated sheeting attached to the purlin provides two main restraining effects, shear stiffness k_{ry} and rotational stiffness k_{rx}. The rotational stiffness comes from both the rotational stiffness of the sheeting itself and the rotational stiffness of the purlin-sheeting connection. The nature of the shear stiffness and the sheeting rotational stiffness is shown in Fig. 2. The magnitude of the shear and rotational stiffness supplied by the sheeting governs the degree to which lateral displacement and rotation of the purlin about its longitudinal axis are restricted. Both shear and rotational stiffness cause a significant increase in the strength of the attached purlin, and neglect of their existence in design can result in highly over-conservative estimates of the purlin load-carrying capacity.

The first model, which will be referred to as the Full Model, incorporates both the purlin and the sheeting, and is hence able to simulate the physical interaction of the two components. The proposed model allows both the membrane and flexural restraining effects of the sheeting to be accounted for, without the need for either experimental input or overly simplifying assumptions. The model uses a nonlinear elasto-plastic finite element analysis, incorporating a rectangular thin-plate element previously developed by Chin, Al-Bermani and Kitipornchai (1994). The loading is applied across the sheeting, as would occur in the physical system, and is transferred to the purlin at the screw connections and at other points of contact between the purlin flange and the sheeting.

The Full Model analysis is compared with experimental results from a test program carried out at the University of Sydney (Hancock et al. (1990,1992), Rousch and Hancock (1995)), in order to show the validity of the model. Single, double and triple span purlins under both uplift and downwards loading are considered.

While the comparison with experimental data shows the Full Model to be a valid tool in predicting the behaviour of the purlin sheeting system, it requires both a large amount of computer memory and considerable running time. For this reason, a simplified version of the model, which is more suitable for use in a design environment, was developed. This model is referred to as the Simplified Model.

The Simplified Model includes purely the purlin and represents the restraining action of the sheeting by placing springs at each centre flange node, the positions at which the purlin is connected to the sheeting (Fig. 3). The restraint provided by the sheeting to the purlin takes two forms, shear stiffness (k_{ry}) and rotational stiffness (k_{rx}), as were previously defined. Both these effects are included in the Simplified Model by augmenting the appropriate terms in the stiffness matrix of each element containing a centre flange node. The Simplified Model requires the stiffness of the sheeting as input, but provides tools to determine both the shear and rotational stiffness of any system numerically. It is accompanied by tables giving values for common purlin and sheeting configurations. The Simplified Model thus avoids the need for either over-conservative simplifications or experimental input.

Experimental results from the University of Sydney test program are used to show the validity of the Simplified Model. Single, double and triple span purlins under both uplift and downwards loading are considered.

2 PREVIOUS RESEARCH

The purlin-sheeting system has been the subject of numerous theoretical and experimental investigations over the past thirty years, but the complexity of the problem has led to great difficulty in developing a sound and general model. The complexity shows itself in two main areas. Firstly, the purlin is either a channel or zed section and is therefore not doubly symmetric as in common beam design. The purlin undergoes significant cross-sectional distortion from the onset of loading. Secondly, the nature of the purlin-sheeting connection makes the shear and rotational stiffness provided by the sheeting to the purlin difficult to quantify. The rotational stiffness, in particular, varies with sheeting type, purlin type and dimensions, screw spacing, and other connection details. The approach in dealing with these

complexities has often been to neglect the effects of purlin cross-sectional distortion and/or the effect of the rotational restraint provided by the sheeting. The assumption that the purlin fails in a mode of flexural-torsional buckling has also frequently been made.

A comprehensive experimental program was carried out at the University of Sydney from 1989-1995 using a vacuum test rig. The test rig consisted of a sequence of three or four evenly spaced purlins screw connected to corrugated sheeting, with the vacuum simulating either uplift or downwards loading. A variety of purlin sections was tested using common sheeting profiles. Single, double and triple span configurations were tested, with and without intermediate bridging. The results from this test program are reported in the papers by Hancock et al. (1990,1992) and Rousch and Hancock (1995).

The tested purlins under wind uplift were found to fail suddenly by localised failure at the free flange-web junction, the free flange lip-stiffener or across the full width of the free flange. The lapped continuous purlins under downwards load were all found to fail by a mode of localised failure at the end of the lap. In no cases was flexural-torsional buckling significantly visible.

3 FINITE ELEMENT ANALYSIS

The finite element analysis used in the Full Model is based on a thin-walled rectangular plate element, initially formulated by Chin, Al-Bermani and Kitipornchai (1994). This analysis is capable of accurately predicting the nonlinear behaviour of plate structures, accounting for cross-sectional distortion, local instability and yielding.

4 DEVELOPMENT THE FULL MODEL

4.1 Purlin-Sheeting Interaction

Fig. 1 shows the behaviour of channel and zed section purlins under uplift loading. The channel section tends to rotate around the middle of the flange where the screw connection is located, while the zed section tends to rotate around the upper flange-web junction. In both cases, the sheeting exerts a retarding effect on the purlin rotation, both at the screw connection and at all other points of contact. These 'points of contact' can be thought of as nodes with dependent degrees of freedom. The lateral w and vertical v deflections, and in some cases rotation q_x, of the sheeting and purlin nodes at these contact points can be related, either by a direct equality expression or by some other linear function. An effective way of incorporating these relationships (or constraints) is by use of Lagrange Multipliers (Cook (1981)), a method in which the stiffness matrix of the structure is modified in order to enforce prescribed relationships that couple dependent degrees of freedom.

In a full scale roof system, a series of purlins would run parallel to each other with continuous lapped sheeting spanning the roof. In the Full Model, a single purlin is modelled with sheeting the width of one span between the purlins, as shown in Fig. 4. The continuous nature of the sheeting is modeled by incorporating appropriate boundary conditions.

4.2 Failure Criterion

Due to the restraint provided by the sheeting to the attached flange of the purlin, purlins fail by a combination of local plastic collapse, local buckling and yielding, rather than by overall buckling. For the purlins analysed using the Full Model, once plastification was reached (generally in the free flange region near the midspan of the purlin) very small load steps were used until the solution failed to converge in the set number of iterations. This divergence of the solution, occurring shortly after plastification commenced in the purlin, was taken as indicating purlin failure and the load at which this occurred was taken as the predicted failure load.

4.3 Comparison of the Full Model with Experimental Results

In order to verify the accuracy of the Full Model, the response predicted by the model is compared with experimental results from the Vacuum Test Rig Program carried out at the University of Sydney. Information regarding the Test Program is given in the papers by Hancock et al. (1990,1992) and Rousch and Hancock (1995). Single, double and triple span purlins were tested and comparison with the Full Model for purlins of each of these configurations is presented in this section.

4.3.1 Single Span Purlins

Tests S7T1, S7T2, S7T3 and S7T5 were carried out on simply supported 7m purlins attached to a 1400mm width of Spandek Hi-Ten sheeting (Lysaght Building Industries (1991)) under uplift loading. The details of these tests are briefly outlined below:

Test S7T1	Span: 7m	Section:	Z200-15	No. Rows Bridging:	0
Test S7T2	Span: 7m	Section:	C200-15	No. Rows Bridging:	0
Test S7T3	Span: 7m	Section:	C200-15	No. Rows Bridging:	1
Test S7T5	Span: 7m	Section:	C200-15	No. Rows Bridging:	2

Table 1 presents the comparison of the experimental results with the failure loads predicted by the Full Model analysis. The analysis shows very good agreement with the experimental results, the ratio of model to test failure loads ranging from 0.96 to 1.00. Tests S7T1 and S7T2, the unbridged purlins, when analysed using the Full Model, commenced yielding in the lower flange elements nearest the web, 350mm from the centre of the purlin. The tested purlins failed by local plastic collapse of the free flange in a similar location.

The analysis of S7T3, the purlin with one row of bridging located at midspan, indicated that yielding started at midspan in both lower flange elements and in the lower lip element. The tested purlin failed by collapse across the whole bottom flange, also at midspan. Test S7T5, the purlin with two rows of bridging, failed by both lip stiffener buckles near the quarter points of the purlin as well as local plastic collapse of the free flange at midspan. The Full Model analysis of this purlin showed the onset of yield occurring in the lip element 1925mm from the end of the purlin, very near the location of the lip stiffener buckles.

4.3.1.1 Load-deflection response

The Full Model is also able to predict the load-deflection response of the purlins. The vertical and lateral deflections of the unbridged purlins of test S7T2 are shown in Figs 5a and 5b, respectively. Figs 6a and 6b show the vertical and lateral deflections of purlins in test S7T5, these purlins having two rows of bridging. The deflections given in these figures were measured at the lower flange-web junction of the purlins at midspan. Gauges were placed on each of the purlins in the test setup, 1 being the purlin at the bottom of the test frame (curve M1 in the figures), 2 being located in the middle (curve M2 in the figures) and 3 being the purlin at the top of the frame (curve M3 in the figures). The lateral deflection of the purlins is taken to be positive when it takes the form shown in Fig. 1.

In general the analysis shows good correlation with the measured deflections. Some discrepancy between the predicted and measured values, as seen in the figures, is to be expected due to initial imperfections in the purlins, follower force due to the vacuum loading (the applied load from the vacuum acts normal to the deformed sheeting while the direction of the applied load in the analysis remains normal to the initial undeformed plane of the sheeting) and movement in the screw connection during loading. No information was available in order to assess the influence of any of these variables. The agreement between the measured and predicted response is therefore felt to be adequate.

Figs 7a-7d show the deflected shape of the purlin cross-section at midspan, as determined by the Full Model analysis at various load levels. They indicate the large degree of cross-sectional distortion experienced by the purlin during uplift loading and also the difference in the response of the unbridged zed section purlin (Fig. 7a) to that of the unbridged channel section purlin (Fig. 7b). Comparing the lateral deflections of the purlins in tests S7T3 (one row of bridging) and S7T5 (two rows of bridging), which are given in Figs 7c and 7d, with the lateral deflection of the same channel section in an unbridged configuration (S7T2, Fig. 7b) indicates that the lateral deflection of the purlin is significantly reduced by the presence of bridging.

The normal and lateral deflections along the length of the purlin, calculated using the Full Model, have been investigated. The overall responses of the unbridged zed and channel section purlins are very similar while the bridging in sections S7T3 with one row of bridging and S7T5 with two rows of bridging clearly decreases the lateral deflections of the purlin, while having a lesser effect on the normal deflections.

4.3.2 Double Span Purlins

Continuous zed section purlins consisting of two 10.5m spans were tested under uplift loading in tests S2T1, S2T2 and S2T3. These purlins were arranged at 1200mm centres and attached to either Monoclad (Stramit Industries (1993)) or Trimdek (Lysaght Building Industries (1991)) sheeting. Details of these tests are briefly summarised here:

Test S2T1	Span: 10.5m	Section:	Z300-25	No. Rows Bridging:	0
Test S2T2	Span: 10.5m	Section:	Z300-25	No. Rows Bridging:	1
Test S2T3	Span: 10.5m	Section:	Z300-25	No. Rows Bridging:	2

The three tested purlins failed by local plastic collapse at the flange-web junction near the centre of the purlin, along with inner flange general failure at the end of the lap in the third test. The purlins, when analysed using the Full Model, all commenced yielding in the lower flange element closest to the web. This element was located at the division closest to the end of the lapped region of the purlin. The load at which the tested purlins failed is compared with the failure load predicted by the Full Model in Table 1. All predicted loads are within 5% of the experimental result.

4.3.3 Triple Span Purlins

Four purlins are presented in this section for comparison with the analytical model, two under uplift loading (Test S1T4 and Test S1T5) and two under downwards loading (Test S4T5 and Test S4T6). The details of these tests are briefly given below (where U indicates uplift loading and D indicates downwards loading).

Test S1T4	Span: 7m	Section:	Z200-15	No. Rows Bridging:	0 (U)
Test S1T5	Span: 7m	Section:	Z200-15	No. Rows Bridging:	1 (U)
Test S4T5	Span: 7m	Section:	Z150-19	No. Rows Bridging:	0 (D)
Test S4T6	Span: 7m	Section:	Z150-19	No. Rows Bridging:	1 (D)

In each case the purlin is made up of three spans, lapped over the internal supports and attached to 1200mm spans of Monoclad or Trimdek sheeting.

Comparison of the failure loads of the tested purlins and those predicted by the Full Model are presented in Table 1. For both the uplift and downwards loading cases, the model predicts within 5% of the tested purlin failure load.

5 DEVELOPMENT OF THE SIMPLIFIED MODEL

While the Full Model offers an excellent tool for the understanding of the purlin-sheeting system, it is computationally quite demanding which would tend to impede its use in regular design situations. A simplified version of this model was therefore developed, which, while not offering the advantage of including both the sheeting and purlin, is less computationally demanding and is therefore more appropriate for use in standard design.

5.1 Shear Stiffness

The shear restraint provided by the sheeting to the purlin is primarily independent of the purlin profile but does vary with both sheeting type and span. As part of the Simplified Model, a numerical tool, the Double Beam Shear Test (DBST) Model, was developed to determine the shear stiffness of various sheeting profiles. Using this model, the variation of shear stiffness with sheeting span and sheeting type was considered. The sensitivity of purlins to the value of sheeting shear stiffness was investigated and a single value of stiffness proposed for standard purlin-sheeting systems. The following sections outline this procedure.

5.1.1 Double Beam Shear Test

Pincus (1963) developed a test to determine the shear restraint provided by the sheeting to the purlin, referred to as the Double Beam Shear Test. This test can be modeled using similar discretisation and constraint conditions as in the Full Model in order to determine the shear stiffness of a particular sheeting type and configuration.

The standard spans of sheeting commonly used in Australia range in 300mm increments from 900mm to 3300mm. The DBST model was used to determine the shear stiffness of four standard corrugated sheeting profiles over this range of spans. The dimensions of these sheeting profiles (Spandek Hi-Ten and Trimdek) are presented in Fig. 8. The results of DBST Model analysis are shown in Fig. 9. The shear stiffness of the sheeting increases with both sheeting thickness and sheeting span.

5.1.2 Sensitivity of Purlin to Shear Stiffness

Many of the previous models of the purlin-sheeting system assumed that the sheeting provided complete restraint against lateral deflection of the purlin, that is, had infinite shear rigidity (Ings and Trahair (1984), Peköz and Soroushian (1982) for example). Others, such as those presented by Pincus (1963) and Davies (1976), determined the shear stiffness for each individual case using purely experimental or experimental-empirical approaches.

In order to decide the approach to adopt in the Simplified Model, it was necessary to first investigate the sensitivity of the purlin to the value of shear stiffness provided by the sheeting. Assuming a constant value of rotational stiffness (determined for the particular purlin in the manner described in a later section), both a zed and channel section purlin were analysed using the Simplified Model, considering a range of shear stiffness from 0 to 100,000 kN/rad. The purlins investigated had a single span of 7m, the zed section being a Z200-24 profile purlin and the channel section being a C200-24 profile purlin. Figure 10 shows the normal deflections of the purlins at an uplift load of 1kN/m for the range of shear stiffness. The deflections are measured at the compression flange-web junction of the purlin at midspan. The terms in brackets indicate the load (in kN/m) at which the purlin first yields. This yield occurs at the lower flange-web junction, near the centre of the purlin.

From Fig. 10 it can be seen that the zed section purlin is particularly sensitive to the value of shear stiffness while the channel section is not strongly influenced by its effect. Over the range from 300 kN/rad to 100,000 kN/rad, neither purlin shows a strong decrease in deflection or any significant increase in strength. Fig. 9 shows that the shear stiffness for common sheeting profiles ranges from approximately 300 kN/rad to 1500 kN/rad, that is, within the range in which the purlin is not significantly sensitive to any increase in shear stiffness. It was therefore decided to adopt a 'standard' value of 1000 kN/rad to represent the shear stiffness of the common sheeting profiles.

5.2 Rotational Stiffness

The rotational restraint provided by the sheeting to the purlin is a complex parameter, varying with each purlin-sheeting combination. Unlike the case of shear stiffness, the purlin is sensitive to the value of rotational restraint within the range of commonly used sheeting

profiles. In the following section, this sensitivity of the purlin will be investigated. A numerical tool, the Rotational Restraint (RR) Model, will then be developed and used to determine the rotational stiffness of a number of different sheeting configurations. The variation of rotational stiffness with sheeting profile and span will be investigated. The rotational restraint provided by standard sheeting types to commonly used purlin profiles will be determined and a chart developed from which this value of stiffness can be read.

5.2.1 Sensitivity of Purlin to Rotational Stiffness

Fig. 11 shows the normal deflections of both a zed (Z200-24) and a channel (C200-24) section purlin for a range of rotational stiffness from 0 to 100,000 N/rad. The 7m span purlin is assumed to be attached to sheeting providing a shear stiffness of 1000kN/rad. The deflections are plotted at an uplift load of 1kN/m and are measured at the purlin compression flange-web junction at midspan. The load (in kN/m) at which the purlin first yields is shown in brackets. Values of rotational restraint commonly vary from around 200 N/rad to around 4000 N/rad. Within this range of values, both the channel and zed section purlins are sensitive to changes in rotational stiffness. Therefore, a standard value of rotational stiffness cannot be adopted and a procedure for determining the stiffness must be developed.

5.2.2 Rotational Restraint Model

A test known as the Torsional Restraint Test, shown in Fig. 12, has been adopted by a number of researchers (for example Rousch and Hancock (1994)) as a means to determine the rotational restraint the sheeting provides to the purlin. A modified version of the Torsional Restraint Test can be modeled using the techniques described for the Full Model. This model (referred to as the Rotational Restraint (RR) Model) can be used to determine the rotational restraint provided purely by the sheeting to the purlin and the calculated value used as input for the Simplified Model.

5.2.3 Variation of Rotational Stiffness with Sheeting Profile and Span

Using the RR Model, the rotational stiffness provided by four different sheeting profiles to a zed (Z200-15) and a channel (C200-15) section purlin was determined. The four sheeting profiles were 0.42mm thick Trimdek, 0.42mm thick Spandek, 0.48mm thick Trimdek and 0.48mm thick Spandek (Lysaght Building Industries (1991)). All profiles had a span of 1200mm. The calculated stiffness for each of these combinations is given in Table 2a. For both the zed and the channel section purlin there is only a twelve percent difference between the stiffness provided by the four different profiles, a difference which would have no significant effect on the strength of the purlin. For purlins of the same sectional dimensions, the zed section was always found to receive greater rotational restraint from the sheeting.

The effect of sheeting span on the rotational stiffness provided by the sheeting was found to be very minor. The rotational stiffness provided by 0.42mm Trimdek to a purlin of section Z200-15 was calculated using the RR Model for a range of sheeting spans from 900mm to 3000mm. The results of this analysis are given in Table 2b. The value of rotational stiffness varied by only one percent for the range of sheeting spans.

5.2.4 Rotational Stiffness for Common Purlin Profiles

In Australia, a number of standard purlin profiles are available with manufactures producing charts of allowable design loads for these particular sections. The purlins are generally referred to in a form such as Z200-24 in which the 'Z' indicates a zed section, 200 gives the mean depth of the purlin in mm and 24 indicates an average thickness of 2.4mm. The rotational stiffness provided by a 1200mm span of 2 different sheeting types (Trimdek and Spandek) was determined for each of the common purlin profiles, using the RR Model and the results of this analysis are shown in Figs 13 and 14.

Despite their quite different profiles and thicknesses, Trimdek and Spandek provide very similar restraint to a particular purlin. In subsequent use of the Simplified Model, therefore, the stiffness determined for 0.42mm thick Trimdek (Fig.13) will be taken as representative of all standard sheeting configurations. If the purlin-sheeting system being analysed involves a significantly different sheeting type, purlin type or configuration, the RR Model can be used to determine a system-specific value of rotational stiffness. This value can then be used as input in running the Simplified Model.

5.3 Comparison of Simplified Model with Tested Purlins

As with the Full Model, experimental results from the Vacuum Test Rig Program carried out at the University of Sydney were used to verify the accuracy of the Simplified Model. Details of the 26 tests carried out in this program are given in the papers by Hancock et al. (1990,1992) and Rousch and Hancock (1995).

5.3.1 Comparison of Purlin Failure Loads

The Simplified Model was used to analyse each of the 26 tested purlins included in the University of Sydney Program. The shear and rotational stiffness values required for the running of the Simplified Model were determined in the manner outlined previously. That is, the shear stiffness k_{ry} was taken as 1000kN/rad for all tested cases, while the value of rotational stiffness k_{rx} for each purlin type was read from Fig. 13.

The failure loads determined using the Simplified Model are presented in Table 3a (single span purlins), Table 3b (double span purlins) and Table 3c (triple span purlins), along with the results from the experimental program. All single and double span purlins were tested under uplift loading, while one of the triple span series (Tests S4T1-S4T6), was tested under downwards loading.

The purlins presented in Table 3 include both channel and zed section purlins with zero, one and two rows of bridging. The purlins have single, lapped double and lapped triple span configurations, and both uplift and downwards loading cases are included. For this wide range of purlins, the Simplified Model predicted within ten percent of the experimental failure load in every case. The average ratio between the Simplified Model result and the experimental result was 1.01, with a standard deviation of 0.05. Given the uncertainty inherent in experimental data (for example, no information was available in order to assess initial imperfections in the purlins or follower force due to vacuum loading), the Simplified Model shows excellent correlation with the test results with respect to ultimate failure load.

5.3.2 Load-Deflection Response

As for the Full Model, the Simplified Model can be used to predict the load-deflection path of the purlin. Fig. 5a (normal deflections) and Fig. 5b (lateral deflections) show this predicted response for the purlins of test S7T2. This test involved single span, C200-15 purlins under uplift loading and the deflections predicted by both the Full and Simplified Models are included in the figures. The load-deflection responses demonstrate the good correlation between the Simplified Model and both test results and results from the Full Model.

The tested purlins tended to fail in a mode involving the free flange of the purlin, whether this took the form of local plastic collapse of the flange or general flange failure. As in the case of the Full Model, the Simplified Model tended to show this failure by indicating that elements in the free flange had yielded at locations approximately matching the location of the tested purlin flange collapse. In order to further investigate the behaviour predicted by the Simplified Model near the failure load of the purlin, contour plots were made of the deflected shape of the free flange. The deflections were determined relative to the deflection of the centroidal line of the purlin, in order to show the localised effects. Two triple span purlins are used to demonstrate this approach, with plots given for a number of load levels up to failure. When plotting the deflected shape of the free flange of these purlins, only half the length of the flange is shown. In these figures a coordinate of zero indicates the simply supported end, while the internal support is located 7000mm from this simply supported end, and the coordinate of 10500mm is the middle of both the purlin and the internal span.

Tests S1T4 and S1T5 involved triple span Z200-15 purlins under uplift loading with no bridging and one row of bridging, respectively. These purlins were both reported to have failed by local plastic collapse of the free flange, approximately 2100mm from the simply supported end. Test S1T5 was also found to have a lip stiffener buckle just after the first row of bridging; this bridging being located 3500mm from the simply supported end. Figs 15 and 16, for the unbridged and singly bridged purlins, respectively, show the development of instability in the free flange between 1000mm and 2000mm from the simply supported end of both these purlins. Figure 16 also shows the instability noted in the tests just after the first row of bridging.

6 CONCLUSION

Two models for predicting the behaviour of purlin-sheeting systems have been presented in this paper. Both models allow for the shear and rotational restraining effects of the sheeting to be incorporated into the analysis, without requiring over simplifying assumptions or experimental input. The use of the thin plate elements allows cross-sectional distortion of the purlin to be included in the analysis and the models are able to determine the ultimate load of a purlin, whether this occurs by yielding or by local buckling.

The first model, the Full Model, incorporates the purlin and the sheeting as an integrated system and hence allows for physical interpretation of the restraint provided by the sheeting to the purlin as well as investigation of the sheeting behaviour. The Simplified Model, which models only the purlin, offers a computationally less demanding alternative which is more

appropriate to standard design. The validity of both models was shown by their good correlation with experimental results.

REFERENCES

Chin, C. K., Al-Bermani, F. G. A. & Kitipornchai, S. (1994), Nonlinear analysis of thin-walled structures using plate elements. *International Journal for Numerical Methods in Engineering*, 37, pp. 1697-1711.

Cook, R. C. (1981), *Concepts and Applications of Finite Element Analysis*. 2nd edn, John Wiley and Sons, New York.

Davies, J. M. (1976), Calculation of steel diaphragm behaviour. *Journal of the Structural Division, ASCE*, **102** (7), pp.1411-1430.

Hancock, G. J., Celeban, M., Healy, C., Georgiou, P. N. & Ings, N. L. (1990), Tests of purlins with screw fastened sheeting under wind uplift. *Proc., Tenth International Specialty Conference on Cold-Formed Steel Structures*, University of Missouri-Rolla, St. Louis, Missouri, USA, pp. 393-419.

Hancock, G. J., Celeban, M. & Healy, C. (1992), Tests of continuous purlins under downwards loading. *Proc., Eleventh International Specialty Conference on Cold-Formed Steel Structures*, University of Missouri-Rolla, St. Louis, Missouri, USA, pp. 157-179.

Ings, N. L. & Trahair, N. S. (1984), Lateral buckling of restrained roof purlins. In *Thin-Walled Structures*, vol. 2, ed. J. Rhodes, Elsevier Applied Science Publishers, England, 4, pp. 285-306.

Lysaght Building Industries (1991), *Design Manual: Steel Roofing and Walling*.

Peköz, T. & Soroushian, P. (1982), Behaviour of C- and Z- purlins under wind uplift. *Proc., Sixth International Specialty Conference on Cold-Formed Steel Structures*, University of Missouri-Rolla, St. Louis, Missouri, USA, pp. 409-429.

Pincus, G. (1963), The performance of columns and beams continuously braced with diaphragms. PhD Thesis, Cornell University.

Rousch, C. J. & Hancock, G. J. (1994), A non-linear analysis model for simply-supported and continuous purlins. *Research Report R688, School of Civil and Mining Engineering, The University of Sydney*.

Rousch, C. J. & Hancock, G. J. (1995), Tests of channel and Z-section purlins undergoing non-linear twisting. *Research Report R708, School of Civil and Mining Engineering, The University of Sydney*.

Stramit Industries (1993), *Monoclad: High Strength Roof and Wall Cladding*.

TABLE 1

Full Model and Test Failure Loads

Test	Failure Load Test (kN/m)	Failure Load Full Model (kN/m)	Ratio (Analysis/Test)
Single Spans			
S7T1	1.85	1.87	1.01
S7T2	1.70	1.65	0.97
S7T3	1.70	1.64	0.96
S7T5	1.95	1.95	1.00
Double Spans			
S2T1	4.33	4.23	0.98
S2T2	4.93	4.87	0.99
S2T3	5.77	5.65	0.98
Triple Spans			
S1T4	2.58	2.60	1.01
S1T5	2.94	2.83	0.96
S4T5	2.92	2.90	0.99
S4T6	2.69	2.81	1.04

TABLE 2

Variation of Rotational Restraint with Sheeting Parameters:
(a) Variation with Sheeting Profile Channel Section: C200-24; Zed Section: Z200-24 Sheeting Width: 1200mm.
(b) Variation with Sheeting Span Zed Section: Z200-15 Sheeting: 0.42mm thick Trimdek

(a)

Sheeting Profile	k_{rx} (N/rad) Channel	k_{rx} (N/rad) Zed
0.42mm Trimdek	753.7	980.8
0.48mm Trimdek	754.6	981.4
0.42mm Spandek	860.6	1104.0
0.48mm Spandek	860.6	1104.0

(b)

Width (mm)	k_{rx} (N/rad)
900	978.9
1200	980.8
1500	982.2
1800	983.5
2100	985.0
2400	986.7
3000	990.0

TABLE 3

(a) Simplified Model and Test Failure Loads, Single Span Purlins

Test Single Span	Section	Span Length (mm)	Rows Bridging/ Span	Failure Load Test (kN/m)	Failure Load Model (kN/m)	Ratio (Model/ Test)
S7T1	Z200-15	7000	0	1.85	1.81	0.98
S7T2	C200-15	7000	0	1.70	1.70	1.00
S7T3	C200-15	7000	1	1.70	1.78	1.05
S7T5	C200-15	7000	2	1.95	1.93	0.99
S3T1	Z200-24	7000	0	3.28	3.59	1.09
S3T2	Z200-24	7000	1	3.69	3.60	0.98
S3T3	Z200-24	7000	2	4.76	4.53	0.95
S3T4	C200-24	7000	0	3.63	3.58	0.99
S3T5	C200-24	7000	1	3.63	3.36	0.93
S3T6	C200-24	7000	2	4.71	4.59	0.97

(b) Simplified Model and Test Failure Loads, Double Span Purlins

Test Double Span	Section	Span Length (mm)	Rows Bridging/ Span	Failure Load Test (kN/m)	Failure Load Model (kN/m)	Ratio (Model/ Test)
S2T1	Z300-25	10500	0	4.33	4.47	1.03
S2T2	Z300-25	10500	1	4.93	5.02	1.02
S2T3	Z300-25	10500	2	5.77	5.75	1.00

(c) Simplified Model and Test Failure Loads, Triple Span Purlins

Test Triple Span	Section	Span Length (mm)	Rows Bridging/ Span	Failure Load Test (kN/m)	Failure Load Model (kN/m)	Ratio (Model/ Test)
S1T1	Z150-19	7000	0	2.31	2.53	1.10
S1T2	Z150-19	7000	1	2.63	2.82	1.07
S1T3	Z150-19	7000	2	2.98	3.07	1.03
S1T4	Z200-15	7000	0	2.58	2.60	1.01
S1T5	Z200-15	7000	1	2.94	2.82	0.96
S1T6	Z200-15	7000	2	3.87	3.91	1.01
S1T7	Z200-19	7000	0	3.51	3.77	1.07
S1T8	Z200-19	7000	1	4.28	3.95	0.92
S1T9	Z200-19	7000	2	4.55	4.30	0.95
S4T1/2	Z200-19	7000	1	3.97/4.42	4.16	0.99
S4T3/4	Z200-15	7000	0	2.90/2.94	2.89	0.99
S4T5	Z150-19	7000	0	2.92	2.94	1.01
S4T6	Z150-19	7000	1	2.69	2.92	1.09

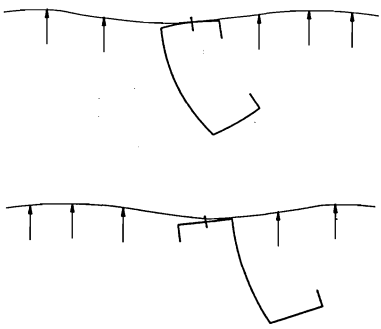

Fig. 1: Deflected shape of purlins under uplift loading

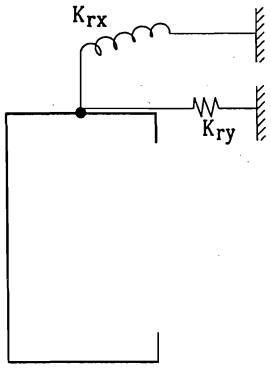

Fig. 3: Modeling of sheeting restraint

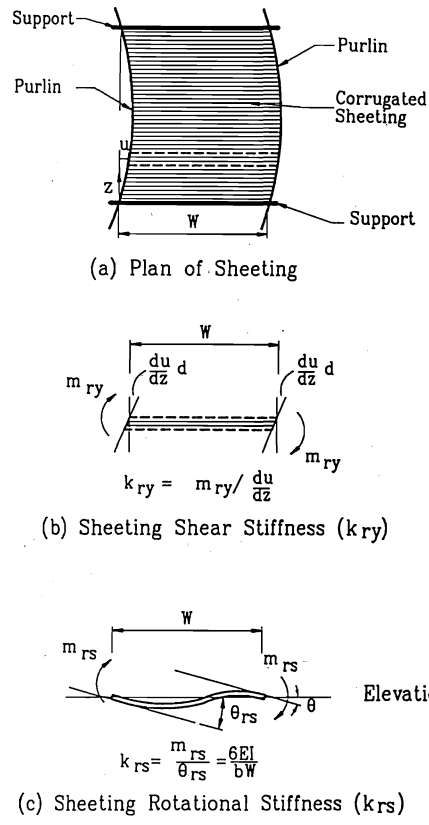

Fig. 2: Sheeting restraint

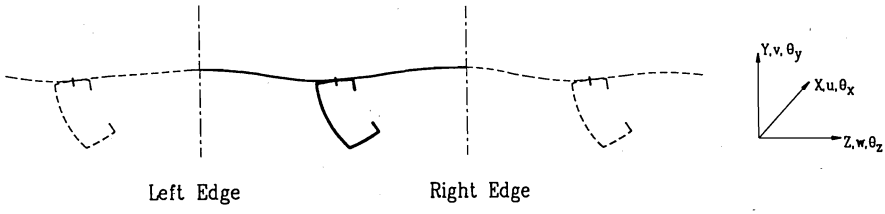

Fig. 4: Section of purlin and sheeting

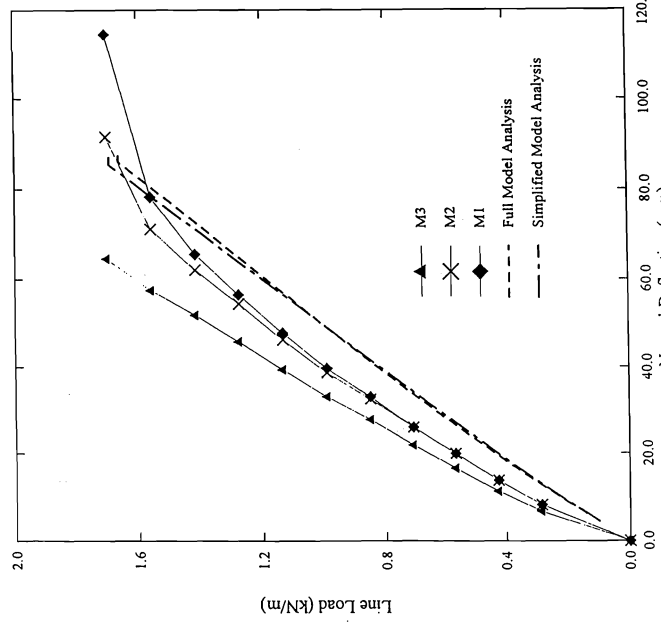

Single Span C200-15 Purlin, Uplift Loading

Fig. 5a: S7T2 Normal deflections midspan

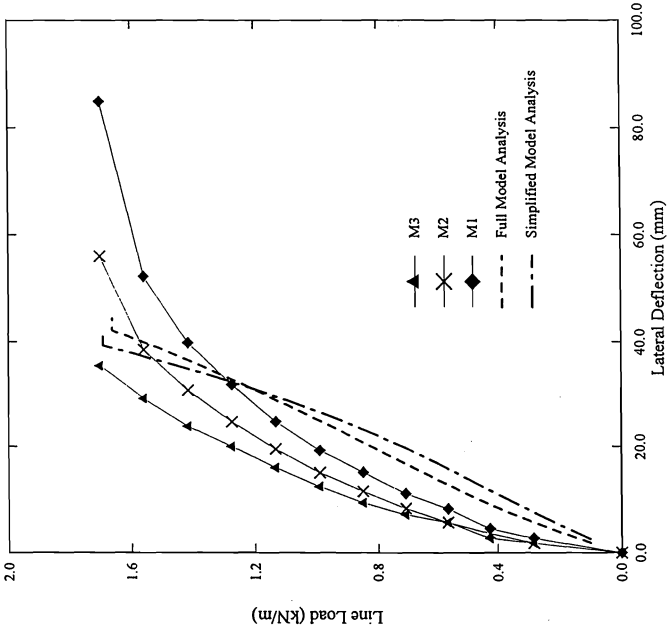

Single Span C200-15 Purlin, Uplift Loading

Fig. 5b: S7T2 Lateral deflection midspan

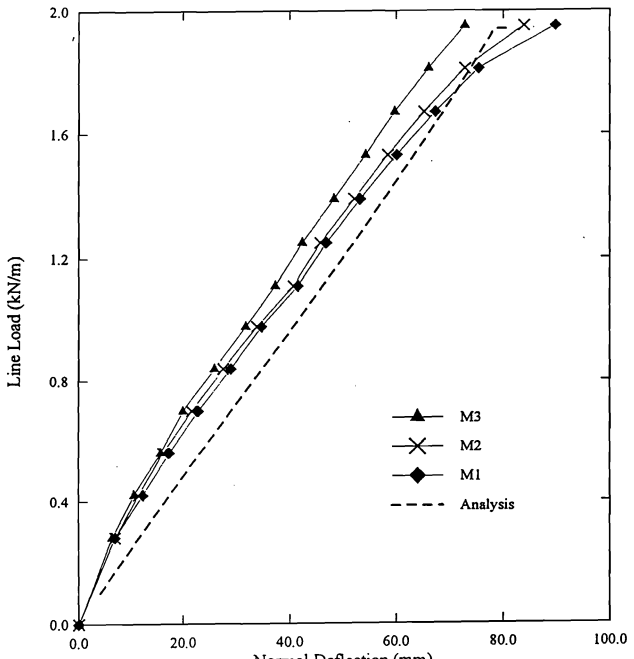

Fig. 6a: S7T5 Normal deflections at midspan

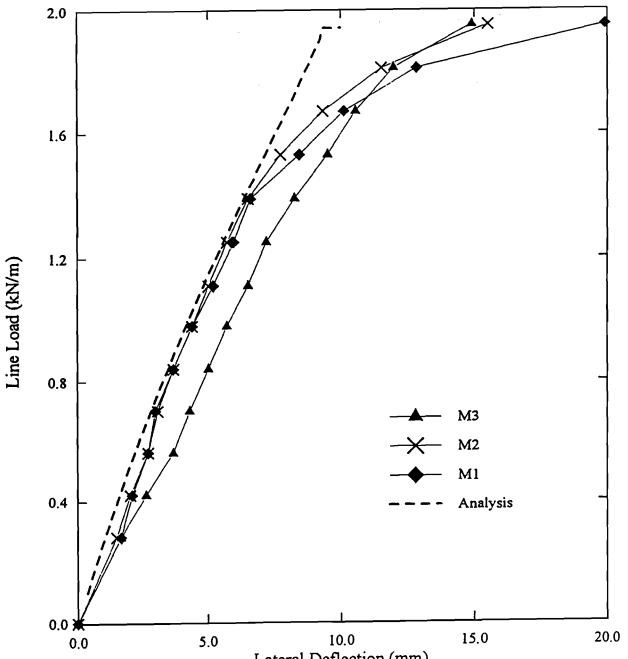

Single Span, C200-15 Purlin, 2 Rows Bridging

Fig. 6b: S7T5 Lateral deflections at midspan

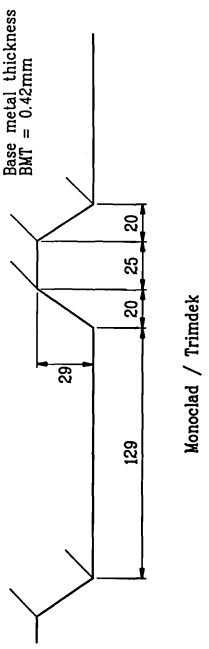

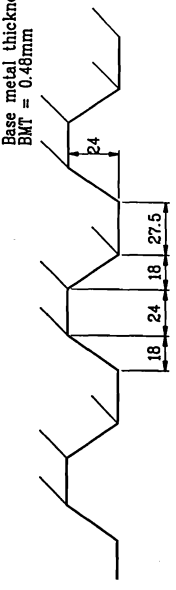

Fig. 8: Basic dimensions of sheeting profiles

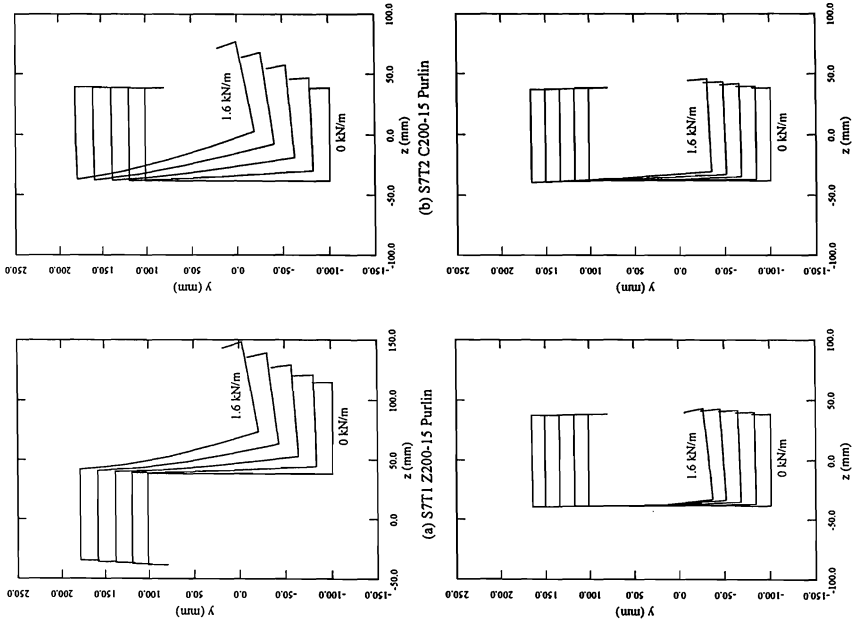

(Plotted at 0.4 kN/m Intervals)

Fig. 7: Deflected shape of single span purlins at midspan

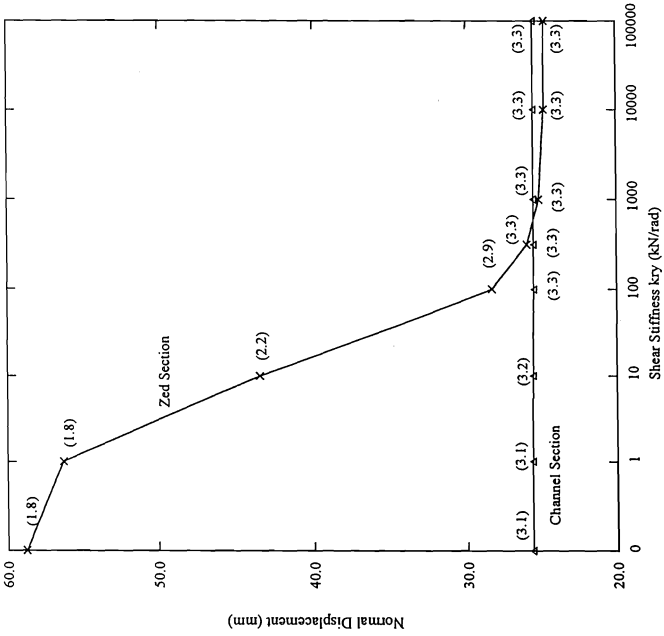

Fig. 10: Normal deflection of purlins with varying shear stiffness

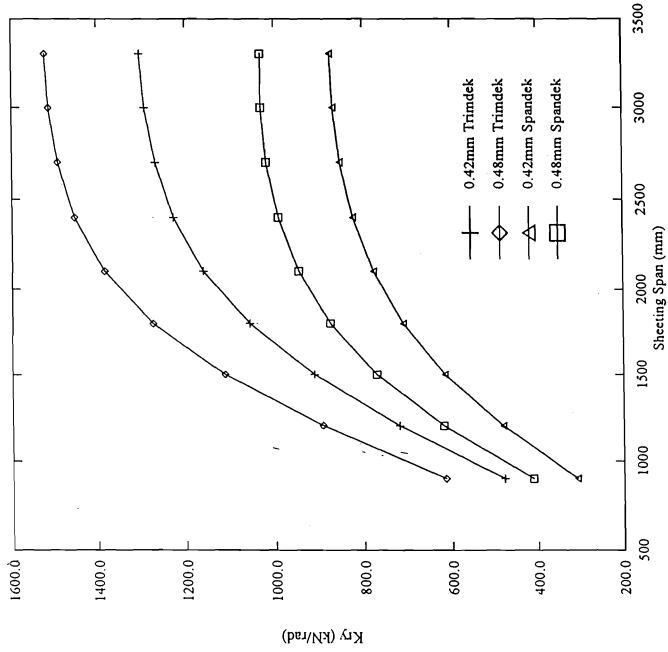

Fig. 9: Shear stiffness for common sheeting profiles

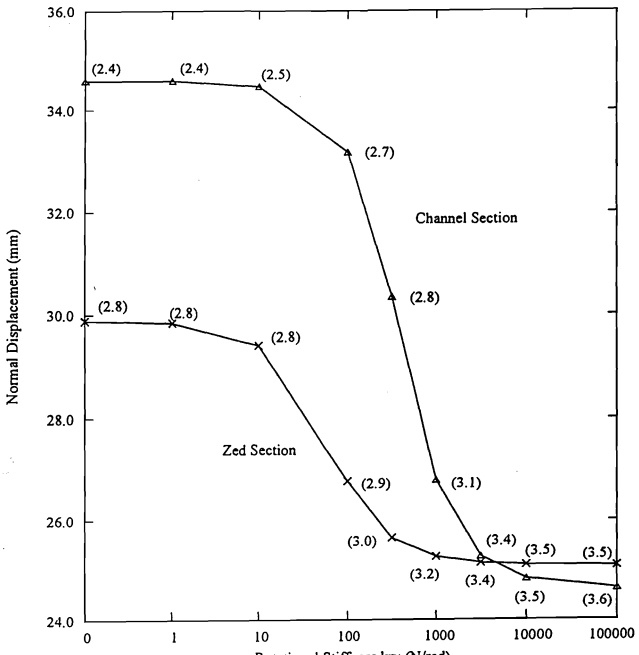

Fig. 11: Normal deflection of purlins with varying rotational stiffness

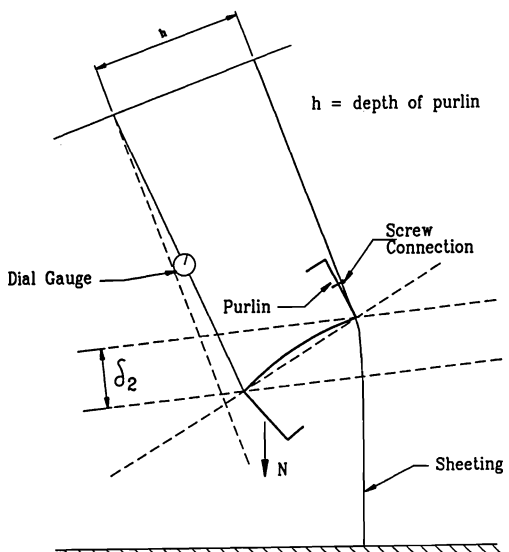

Fig. 12: Torsional restraint test

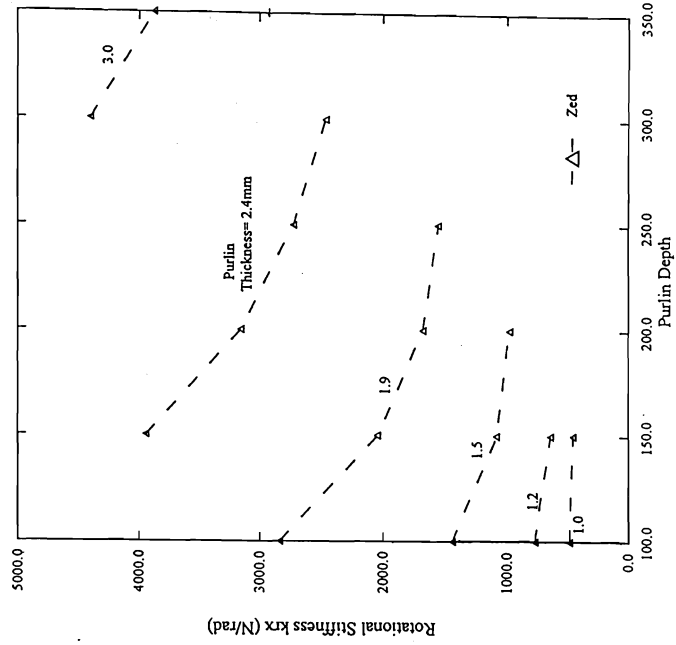

Fig. 13: Rotational restraint for common purlin profiles

Fig. 14: Rotational restraint for common purlin profiles

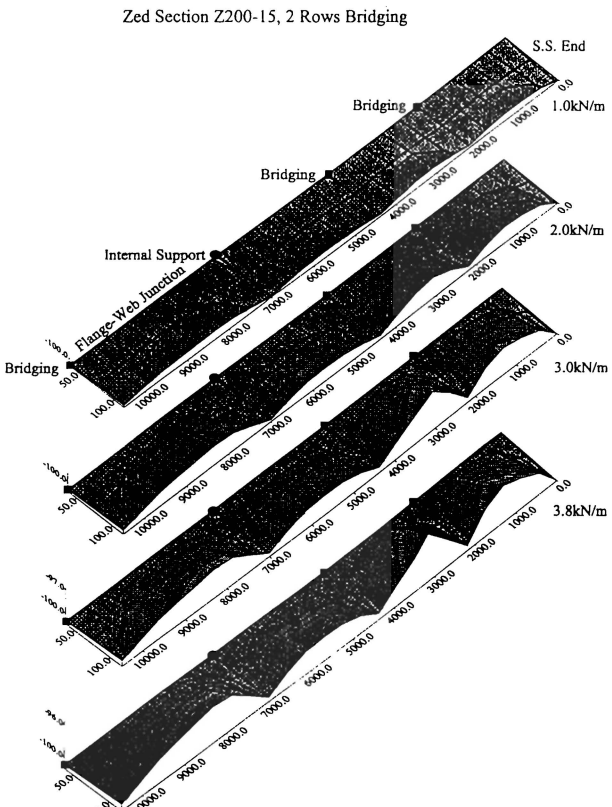

Fig. 15: S1T4 Deflected shape of free flange

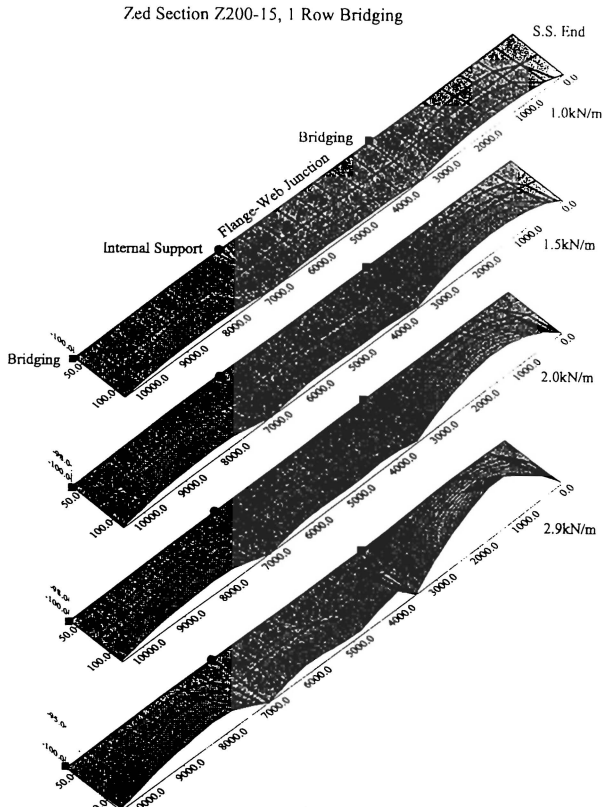

Fig. 16: S1T5 Deflected shape of free flange